INTERNAL DYNAMICS OF PROTEINS

Short Time and Long Time Motions of Aromatic Sidechains in PTI

Martin Karplus, Bruce R. Gelin, and J. Andrew McCammon, *Department of Chemistry, Harvard University, Cambridge, Massachusetts 02138 U.S.A.*

ABSTRACT Theoretical approaches to the internal dynamics of proteins are outlined and illustrated by application to the aromatic sidechain motions of tyrosines in the bovine pancreatic trypsin inhibitor. High frequency torsional oscillations are obtained from a molecular dynamics simulation, while the longer time ring rotations are analyzed by use of adiabatic energy minimization and special transition-state trajectory techniques.

Proteins under native conditions are molecules with considerable internal freedom, in which a wide variety of motions take place (1, 2). These range from the local atomic fluctuations, through sidechain oscillations and group displacements involving secondary and other structural elements to large scale tertiary and quaternary rearrangements; concomitantly, the time scales of motion range from picoseconds to milliseconds or longer. The presence of such motional freedom implies that a native protein at room temperature samples a range of conformations. Most of these are in the neighborhood of the average structure (the x-ray structure corresponds to the average in the crystal), but at any given moment an individual protein molecule is likely to differ significantly from the average structure. Both conformational and energy fluctuations with local to global character are likely to be important. In a protein, as in other nonrigid condensed systems, structural changes proceed through fluctuations and large structural changes arise from correlated fluctuations. Perturbations, such as ligand binding, that produce tertiary or quaternary alterations do so by introducing forces that bias the fluctuations in such a way that the protein makes a transition from one structure to another. Looked at in another way, the fluctuations search out the path or paths along which the transition takes place. The nature of the structure and the transitions may be such that the energy fluctuations play a role in the functional mechanism.

In what follows, we shall outline how protein fluctuations can be studied theoretically. To illustrate the methodology we shall focus on a particular case - the motions of aromatic side chains in the interior of a protein, the pancreatic trypsin inhibitor (PTI). The sidechain motions span a time range from picoseconds, during which local oscillations occur, to milliseconds or longer required for 180° degree rotations. To cover this range of motions requires use of a variety of approaches that complement each other in the analysis of protein dynamics. Their discussion is the main purpose of this paper. Although the aromatic sidechain motions in PTI are in themselves of no biological importance, the results obtained are typical of a wider class of motional phenomena that do play a biological role; e.g., the entrance into and exit from the heme pocket of oxygen in binding to myoglobin and hemoglobin has been

---

Dr. Gelin's present address is the Digital Equipment Corporation, Stanford. Conn.
Dr. McCammon's present address is the Department of Chemistry, University of Houston, Houston, Texas 77004.

shown to require sidechain displacements (3). Further, the methodology used for the aromatic sidechains is applicable to many of the internal motions of interest in protein function.

In any detailed approach to dynamic problems at the atomic level, it is essential to have available the potential energy of the system as a function of atomic coordinates. Although quantum mechanical calculations provide this for small molecules, empirical energy functions of the molecular mechanics type (4–6), are the only possible source of such information for proteins. Since most of the motions that occur at ordinary temperatures leave the bond lengths and bond angles of the polypeptide chains near their equilibrium values, which appear not to vary significantly throughout the protein (e.g., the standard dimensions of the peptide group first proposed by Pauling, et al. [7]), the energy function representation of the bonding can be hoped to have an accuracy on the order of that achieved in the vibrational analysis of small molecules. Where globular proteins differ from small molecules is that the contacts among nonbonded atoms play an essential role in the potential energy of the folded or native structure. From the success of the pioneering conformational studies of Ramachandran and coworkers (8) that made some use of hard-sphere nonbonded radii, it is likely that relatively simple functions (Lennard-Jones nonbonded potentials supplemented by special hydrogen-bonding terms and electrostatic interactions) can adequately describe the interactions involved. The empirical energy function used here is composed of a sum of terms associated with bond lengths, bond angles, dihedral angles, hydrogen bonds, and nonbonded (van der Waals and electrostatic) interactions; hydrogen atoms were included implicitly by a suitable adjustment of heavy-atom parameters. The form and details of the function have been described previously (9, 10).

Given such an empirical potential energy function, two types of approaches to the motions in a protein are possible. The first of these is static in character and can be referred to as the determination of a reaction path, in analogy to what is often done in the study of small molecules and their reactions (11). The second approach is based on solving the classical equations of motion for individual atoms with the set of forces determined from the potential function. The resulting phase space trajectories provide the ultimate detail, as well as appropriate averages, concerning the possible motions. Although small-molecule trajectory calculations (12) and liquid-state molecular dynamics studies (13) are well-known, it is only recently (14) that the equations of motion have been solved for the atoms comprising a protein.

Before undertaking a treatment of the aromatic sidechain dynamics in PTI, we consider the nature of the potential experienced by the sidechains in the interior of the protein. In the native conformation of PTI, the Tyr-21 ring is surrounded by and has significant nonbonded interactions with atoms of its own backbone and of surrounding residues (30, 31, 32, 45, 47, and 48) that are more distant along the polypeptide chains. Fig. 1 shows a potential energy contour map for the sidechain angles χ_1 and χ_2 of Tyr-21 in the free dipeptide (Fig. 1*a*) and in the protein (Fig. 1*b*). The minimum energy conformations are very similar in the two cases; this appears to be true for most interior residues of proteins. Where the plots differ is that the sidechain is much more rigidly fixed in position by its nonbonded neighbors in the protein than it is by interactions with the backbone of the chain. Examination of the details of the nonbonded terms shows that a small number of atoms are involved in constraining the ring in the protein; of particular importance are the backbone N of Ala-48 and $C\gamma_2$ of Thr 32 which are located symmetrically above and below the center of the Tyr-21 ring.

To determine the fluctuations of the aromatic sidechains of PTI a molecular dynamics simulation of the protein was made (10). The dynamics of the 454 heavy atoms of PTI and of

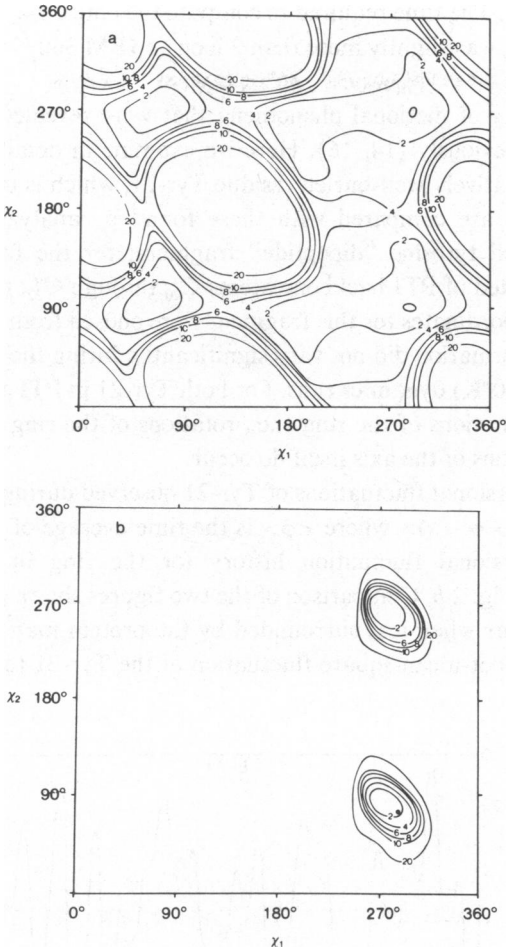

Figure 1 (χ_1, χ_2) maps for Tyr-21: (*a*) free dipeptide; (*b*) peptide in protein; the black dot corresponds to the (χ_1, χ_2) values in the protein (ϕ = 253.23°, ψ = 146.77°, ω = 170.93°); energy contours in kcal/mol.

the four internal water molecules were calculated by numerically integrating the classical equations of motion for these atoms. No constraints were introduced to simplify the system and all of the atoms were allowed to move in accord with the empirical potential function. The integration was performed by means of the fifth-order Gear algorithm (15); a time step of $\Delta t = 9.78 \times 10^{-16}$ s was found to yield accurate results over the time period of the simulation. The simulation was initiated by assigning all atoms in the x-ray structure velocities with equal magnitudes (corresponding to 300°K) and randomized directions. The initial accelerations were computed from the forces acting on the atoms in the x-ray structure; all higher derivatives were initially set to zero. During the first 2.0 ps of the trajectory calculation, the atomic velocities were modified as necessary to maintain the protein temperature at ~300°K and to prevent localized heating due to the nonuniform stresses in the x-ray structure. The equilibration period was continued for an additional 2.9 ps without any external modifications of the atomic velocities to allow more complete relaxation of the protein. The average temperature attained during this period was 308°K. The final phase of the simulation (9.8 ps) provided the trajectory used for statistical analysis; the average temperature during this

period was again 308°K. The time required to compute the entire 14.7-ps trajectory, including the equilibration period, was slightly more than 2 h on an IBM 360/91 computer (IBM Corp., White Plains, N.Y.).

Aspects of the variety of motional phenomena that were revealed by the PTI simulation have been described previously (14, 16). Here we examine in detail the fluctuations of the aromatic ring of the relatively well-buried residue Tyr-21, which is typical of interior protein sidechains. The results are compared with those found by analyzing a simulation of the dynamics of an isolated tyrosine "dipeptide" fragment; for the fragment simulation, the molecular model consisted of PTI backbone atoms C^{α}_{20} through C^{α}_{22}, together with the Tyr-21 sidechain. The initial coordinates for this fragment were chosen from the PTI x-ray structure, and the backbone conformation did not vary significantly during the equilibration (1.2 ps) or analysis (9.8 ps; $T = 280°K$) dynamics runs. For both Tyr-21 in PTI and the Tyr fragment we focus on the torsional motions of the ring (i.e., rotations of the ring plane about the C^{γ}_{21}-C^{ζ}_{21} axis), although oscillations of the axis itself do occur.

Fig. 2 *a* shows the torsional fluctuations of Tyr-21 observed during the PTI simulation; the quantity plotted is $\Delta\phi = \phi - \langle\phi\rangle$ where $\langle\phi\rangle$ is the time average of the ring torsional angle. The corresponding torsional fluctuation history for the ring in the tyrosine fragment simulation is shown in Fig. 2 *b*. Comparison of the two figures shows that the torsional motion of the ring is less regular when it is surrounded by the protein matrix than in the separated fragment. In PTI, the root-mean-square fluctuation of the Tyr-21 torsion angle is 12°, while

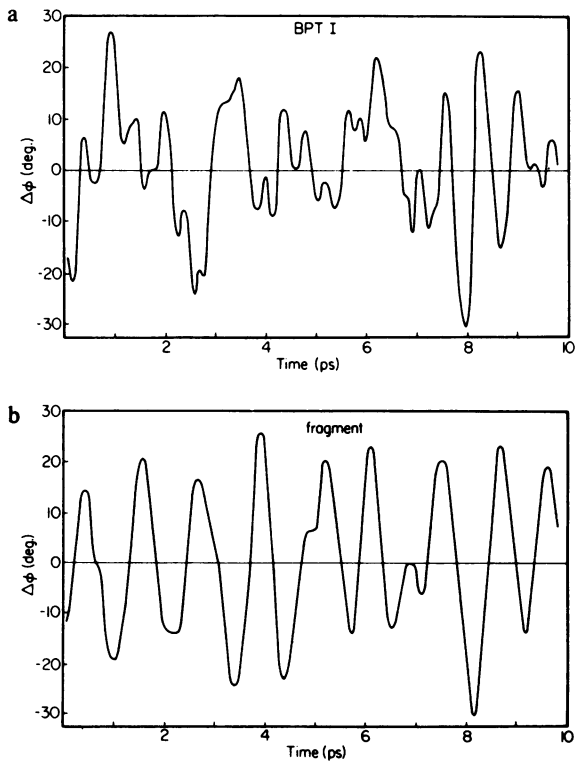

Figure 2 (*a*) Evolution of the Tyr-21 ring torsional angle during the 9.8 ps of dynamical simulation in the protein. (*b*) Evolution of the tyrosine ring torsional angle during 9.8 ps of dynamical simulation of the isolated tyrosine fragment.

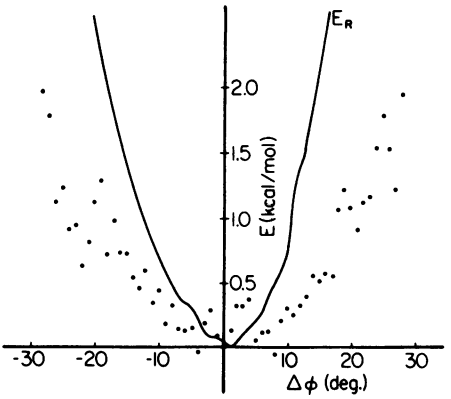

Figure 3 Points represent the potential of mean force for Tyr-21 ring torsional fluctuations, based on statistics from the dynamical simulation. E_R is the total potential energy for Tyr-21 ring torsional displacements in the rigid x-ray structure.

that for the tyrosine fragment is 15°. This relatively small difference in amplitudes as compared with the rigid rotation potential (Fig. 1) makes clear that protein relaxation must play an important role in the ring oscillations. One way of illustrating this is to determine the potential of mean force (17) defined by

$$E(\Delta\phi) = -RT\, lnP(\Delta\phi), \tag{1}$$

where $P(\Delta\phi)$ is the relative likelihood of a fluctuation $\delta\phi$, R is the gas constant, T is the absolute temperature, and $P(0)$ is normalized to 1. The potential of mean force obtained from the PTI simulation is shown in Fig. 3. For purposes of comparison we also show in Fig. 3 a potential, $E_R(\Delta\phi)$, whose shape is determined by rotating the Tyr-21 ring in the rigid x-ray structure. The potential of mean force, $E(\Delta\phi)$, is significantly softer than the rigid-protein potential, $E_R(\Delta\phi)$. Correlation in the displacements of ring and cage atoms in the fluctuating protein thus tend to lower the energy required for a given displacement. An estimate of the typical cage atom displacements which contribute to the softening of the potential of mean force is 0.2 Å, the distance a δ or ϵ ring carbon moves upon a 10° torsional rotation.

Time Correlation Functions

The comparison in Figs. 2 *a* and 2 *b* of the dynamics of Tyr-21 in the protein and as a dipeptide show that the latter behaves much more like an unhindered oscillator than the former. It can be seen that in the protein the aromatic ring undergoes collisions with the surrounding matrix atoms which significantly perturb the ring motion; some of the interactions are sufficiently strong to reverse the direction of motion, while others produce a smaller change in the angular velocity. As expected far fewer of these collisional perturbations are evident in the dipeptide, for which only interactions with the local backbone are included.

To clarify further the dynamic character of the ring fluctuations, it is useful to introduce time correlation functions (18). The time correlation function $C_A(t) = <A(s + t)A(s)>$, for a dynamical variable A is obtained by multiplying the value of $A(s)$ by $A(s + t)$, the value taken by A after the system has evolved for an additional time t, calculating such products for a representative set of initial times, s, and averaging. If the averaging is done over a sufficiently long dynamical simulation of an equilibrated system, $C_A(t)$ will be independent of the initial times, s, used in the calculation; it is then customary to write $C_A(t) = <A(t)A(0)>$. If A is the

fluctuation of a variable from its mean value, $<[A(0)]^2>$ is the mean-square fluctuation of the variable for an equilibrated system, while the time correlation function, $C_A(t)$, describes the average way in which the fluctuation decays. The normalized time correlation function for torsional fluctuations of the Tyr-21 ring in PTI, $C_\phi(t) = <\Delta\phi(t)\Delta\phi(0)>/<[\Delta\phi(0)]^2>$, is shown in Fig. 4 *a*. The torsional oscillations of the ring are seen to be significantly damped. It is apparent that the correlation function contrasts sharply with the continued oscillations expected for an isolated harmonic oscillator. In Fig. 4 *b*, we present for comparison $C_\phi(t)$ calculated from the dynamical simulation of the isolated tyrosine fragment. In this case, the tyrosine ring suffers substantially less damping during its torsional motion; in fact, if the integration is continued for longer times, $C_\phi(t)$ exhibits an oscillatory character with some damping due to the interactions with the backbone.

The form of the correlation function for the torsional motions of the Tyr-21 ring in PTI suggest that it can be described by the Langevin equation for a dampled harmonic oscillator (19):

$$I\frac{d^2\phi}{dt^2} + f\frac{d\phi}{dt} + k\phi = N_r(t). \tag{2}$$

Here ϕ is the torsional coordinate relative to $<\phi> = 0$, $I = 7.5 \times 10^{15}$ g cm^2 mol^{-1} is the moment of intertia of the ring about the torsional axis, f is a friction constant, k is the harmonic restoring force constant, and $N_r(t)$ represents the random torques acting on the ring due to fluctuations in its environment. In using a Langevin equation, we implicitly assume that variations in $N_r(t)$ occur on a much shorter time scale than do variations in ϕ; thus, $N_r(t)$

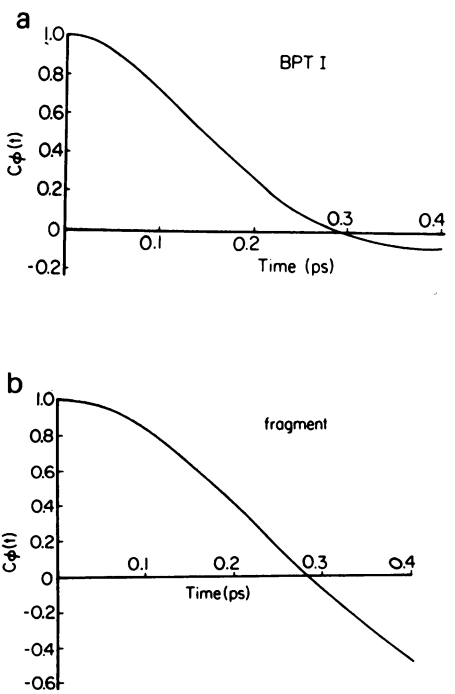

Figure 4 (*a*) The normalized time correlation function for torsional fluctuations of the Tyr-21 ring in the protein, based on molecular dynamics results. (*b*) The normalized time correlation function for torsional fluctuations of the tyrosine ring in the isolated tyrosine fragment, based on molecular dynamics results.

may be regarded as a Gaussian random process and we do not have to specify the mechanism by which the torque fluctuations arise. This time scale assumption is supported by a collisional model in which it is shown that the mean time between significant changes in $N_r(t)$ is ~0.07 ps; reference to Fig. 2 shows that, on the average, ϕ does not change much in this short interval of time. For the restoring force constant, k, it is appropriate to choose a value that includes the effect of cage relaxation. A quadratic fit to the potential of mean force $E(\Delta\phi)$, defined in Eq. 1 yields for Tyr-21 the force constant $k = 5.5 \times 10^{11}$ 1 erg rad^{-2} mol^{-1}; the rigid-protein force constant is $k = 2.2 \times 10^{12}$ erg rad^{-2} mol^{-1}. From Eq. 2 and the definition of relaxation time in the Langevin model, we have $\tau_\phi^L = f/k$. This time is of order of 0.2 ps from Fig. 4 *a*, which yields an estimate of the friction constant $f = k\tau_\phi^L \simeq 0.11$ g cm^2 s^{-1} mol^{-1}. The ratio $f^2/4Ik \simeq 0.74$ is less than unity, indicating that the Tyr-21 ring torsional motions are slightly underdamped (i.e., in the absence of random torques, the ring would relax to its equilibrium orientation by damped oscillations; see reference 19).

The friction constant, f, may be related to an angular diffusion constant by use of the Einstein formula, $D = k_BT/f$, where k_B is the Boltzmann constant and T is the absolute temperature (308°K). For the Tyr-21 ring torsional motion, one obtains $D = 2.3 \times 10^{11}$ s^{-1}. This value is somewhat larger than experimental diffusion constants for the corresponding rotational motion of small aromatic molecules in organic solvents.

Ring Flips

Although the dynamic simulation provides an excellent approach to the small angle oscillations of the tyrosine ring, it does not yield information concerning the probability of ring rotations by 180° (ring "flips"). The latter represent a simple example of an activated process in which the rate is limited by an effective energy barrier. Most processes in native proteins that take place on a time scale of microseconds or longer are likely to involve such an activation step. Measurements have yielded information concerning the free energy barriers associated with a variety of activated processes in proteins; these include the rotations of aromatic side chains (20–22), the motion of diatomic ligands through the globin of heme proteins (23, 24), and the interconversion of substrate and product in enzymes such as triosephosphate isomerase (25). A dynamics simulation of the type described above does not allow one to study activated processes directly because they are by their nature rare events. It is obviously impossible to obtain many barrier crossing trajectories for an activated process with a rate constant of $<10^{11}$ s^{-1} in a simulation of length 10–100 ps.

In one approach to the 180° rotation problem, which is essentially static in character, empirical energy functions are used to estimate the activation barriers (6, 9, 22). In PTI the method has been applied to the 180° rotations of the rings of the eight aromatic sidechains. From the empirical energy function, the analytic gradient (the vector of derivatives with respect to the Cartesian coordinates of all of the extended atoms) can be obtained. This makes it possible to perform energy minimizations via the method of steepest descents in the complete conformational space of the protein.

To evaluate sidechain rotational potentials for the dihedral angle χ(AB–CD) with the rest of the protein fixed rigidly in position, the only atoms displaced are D and those farther from the backbone. Consequently, only a small fraction of the energy function needs to be recalculated for each value of χ and the rotational potential can be determined extremely rapidly. However, such "rigid" rotations can lead to unrealistically high energies as a result of short nonbonded contacts that are easily relieved by small changes in the structure of the protein. To include relaxation effects, the dihedral angle of interest is rotated to a desired

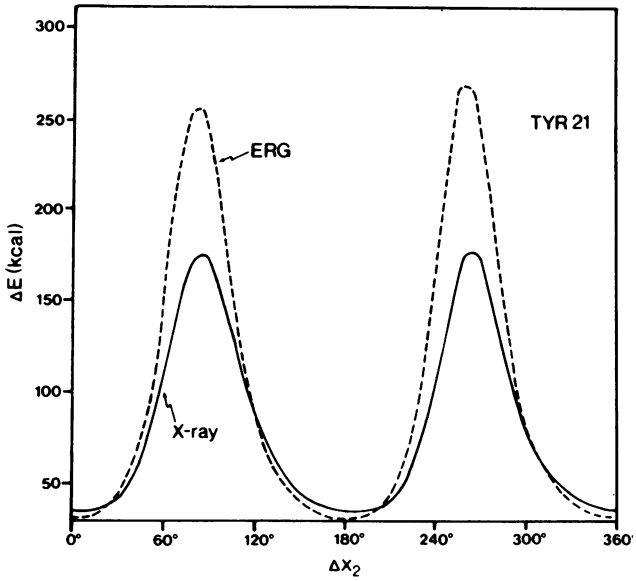

Figure 5 Rigid rotation barriers for the aromatic ring (χ_2) of Tyr-21; both the x-ray and energy-refined geometry (ERG) results are shown.

value and constrained there by a large potential, while all other conformational variables are allowed to change in accord with the steepest-descent procedure (26, 27). Fig. 5 shows the rigid rotation barriers about the ring dihedral angle χ_2 for Tyr-21. The barriers obtained using the x-ray and energy-refined geometry are similar, the latter being slightly higher, as expected. The location of the maximum of the barrier is near 90° and it has an essentially symmetric form.

The rotation barriers found in this way are so large (see Table I) that the protein is not rigid enough to maintain them. Instead, during the rotation of an aromatic ring, it can be expected that "relaxation" of the protein would occur and that the effective barriers would be much reduced. This is made particularly likely by the fact that the dominant contributions to the barriers come from only a few nonbonded contacts (see above). Since such interactions are short range (r^{-12} dependence), a small displacement that costs little in energy can lead to a large reduction in the effective barrier. To evaluate the importance of the relaxation, adiabatic barriers were determined as described. At the minimum ($\Delta\chi_2 = 0°$) and maximum energy orientation of the aromatic ring, 150 steepest-descent cycles of energy minimization were

TABLE I
BARRIER HEIGHTS AND RATE CONSTANTS FOR TYROSINE AROMATIC RING ROTATION

Residue	X-ray geometry barriers	Adiabatic barriers	Reorientation rate constant*
	(kcal/mol)	*(kcal/mol)*	*(s^{-1})*
Tyr-10	22	0	1.2×10^{12}
Tyr-21	140	12	2.5×10^{3}
Tyr-23	63	7	1.0×10^{7}
Tyr-35	175	23	2.7×10^{-5}

*Obtained with Eq. 3 as described in the text.

performed starting with the energy-refined geometry coordinates; this number of cycles appears to be sufficient for convergence of the energy difference between the two orientations (i.e., for the barrier height), although both structures are still slowly decreasing in energy. Table I lists the resulting barriers; Tyr-35 stands out as having the highest barrier value.

The Tyr-21 barrier provides a good example of the mechanism by which steric repulsions are lessened as a result of shifts in atom positions. For a 50-cycle minimization, the barrier is ~15 kcal/mol of which 11 kcal/mol is nonbonded in origin; the bond angle strain is ~5 kcal/mol and all other contributions amount to -1 kcal/mol. The nonbonded part of the barrier has thus been reduced by about ~214 kcal/mol at the cost of 5 kcal/mol in bond angle strain. The additional 100 cycles reduce the barrier by 3 kcal/mol, but do not change the nature of the nonbonded and bond angle strain contributions.

With the barrier results (Table I), it is possible to estimate the rate constant for ring rotation by making a model for the dynamics involved. The simplest assumption is to regard the rotation as a unimolecular process that can be treated by transition state theory, with a classical rate constant k equal to

$$k = \kappa \nu_T e^{-E_A/RT} \tag{3}$$

where ν_T is the vibrational frequency at the bottom of the well and κ the transmission coefficient; for the present calculation, ν_T is estimated to be 1.2×10^{12} s^{-1} and κ is set equal to 1. With this value, the results obtained from Eq. 3 with the adiabatic barriers used for E_A are listed in the last column in Table I. It can be seen that all aromatic residues except Tyr-35 are expected to appear as freely rotating on the time scale of ~1,000 s^{-1} corresponding to the nuclear magnetic resonance measurements, in agreement with the analysis of Snyder et al. (20) and Wuthrich et al (21). Measurements of the temperature dependence of the rate of Tyr-35 have yielded an activation energy of 17 kcal in good qualitative agreement with the barrier calculation (21).

Although static reaction-path studies do provide an approximate value for the energy barrier, they cannot give information concerning the dynamics of the activated process or of the entropic contribution to the rate. To overcome the limitations of standard reaction path and molecular dynamics calculations, a synthesis of these techniques with the widely used concepts of transition state theory can be employed. Such an approach has been applied to small-molecule collision dynamics (28, 29) and more recently to vacancy diffusion dynamics in regular solids (30). The first step in such a calculation is the determination of a transition region in which a dividing surface between reactants and products can be defined. It is then necessary to generate a set of configurations in this region with coordinate values (other than the ones specifying the region) in accord with a Boltzmann distribution for the temperature under consideration. Given the transition-state configurations, two quantities have to be evaluated. The first is the probability that a system composed of reactants at equilibrium will be in the transition region (in transition state theory, this corresponds to the equilibrium constant between the activated complex and the reactants), and the second is the probability that the transition-state configurations with appropriate atom velocities will go on to give product (in transition state theory, this corresponds to the transmission coefficient). Although various aspects of this procedure (sometimes referred to as phase-space/trajectory calculations) can be done analytically in simple cases, the complexity and multidimensionality of a protein reaction requires that the problem be solved numerically by appropriate combinations of Monte Carlo and molecular dynamics techniques. We focus here on the determination of the transition region, the generation of configurations in that region, and the ring reorienta-

tion dynamics of these configurations (31, 32). For specific study we choose Tyr-35 which like Tyr-21 is in the interior of the protein and has been shown to have the highest activation barrier to 180° rotation (see above). Because the rotational barrier is dominated by nonbonded interactions between ring atoms and those of the surrounding protein this case is an ideal example for examining the dynamics of a process in which the effects of protein relaxation and frictional damping are important. The transition state coordinate sets of PTI (i.e., thermodynamically possible configurations, subject to the constraint that the ring be near the top of its rotational potential energy barrier) were prepared in the following manner: a coordinate set was selected from the equilibrium dynamical simulation of PTI, the ring was rigidly rotated to a high energy orientation, and the surrounding protein matrix was allowed to relax by Metropolis Monte Carlo methods, while the ring orientation was held fixed by appropriate constraints. Adjustments of the ring orientation were made by rotation through small angles followed by continued Monte Carlo sampling until trial trajectory calculations resulted in successful barrier crossing. At this point, a longer Monte Carlo calculation was performed to generate transition state configurations for detailed study. To obtain a more adequate coverage of configuration space and to test the adequacy of the Monte Carlo method for generating a representative set of configurations, the whole procedure was repeated starting with a different set from the equilibrium molecular dynamics simulation.

For computing a trajectory which passes through a given transition state configuration, it is necessary to assign initial velocities to the atoms in that configuration; these were chosen from appropriate Maxwellian distributions. With the initial positions and velocities, one half of the trajectory (e.g., the ring falling from the transition state into the final state valley in the potential surface) was calculated by molecular dynamics methods. The other half of the trajectory (e.g., the ring rising from the initial state valley to the transition state) was obtained by using velocities with opposite signs in the initial conditions, calculating the corresponding trajectory and then reversing it in time. Trajectories were calculated for five transition states from each of the two Monte Carlo series, which can be thought of as representing crossings through two local regions of the transition state domain. The equations of motion were integrated by the same method used in the equilibrium dynamics simulations; the total length of each trajectory was 1.17 ps. In every case the ring torsional angle increased monotonically with time during the barrier crossing. However, there are some significant differences in the detailed time variations of the angle. In seven trajectories, the angular motion corresponded to that expected for a simple barrier; that is, the ring slowed down somewhat when it approached the top and then sped up as it moved down the far side. Fig. 6 *a* shows the time variations of the ring torsional angle and torsional angular velocity for one such case. In the other three trajectories, the torsional motion of the ring was nearly stopped one or more times during the barrier crossings; an example is given in Fig. 7 *a*. A detailed analysis shows that the torsional motion of the ring in every trajectory can be accounted for in terms of non-bonded repulsions between ring and protein matrix atoms. More specifically the total impulse due to the resulting torques that exceed 10 kJ/mol in magnitude at any instant is nearly equal to the observed angular momentum change of the ring during the interval over which these torques act. The time variations of all such torques acting during two trajectories are shown in Figs. 6 *b* and 7 *b*, respectively. Analysis of these figures and corresponding ones for the other trajectories shows that most of these torques have substantial magnitudes only for rather short intervals (0.1 ps). From the set of trajectories, it is clear that damping or frictional effects are present but do not dominate inertial effects in the barrier-crossing dynamics. This qualitative

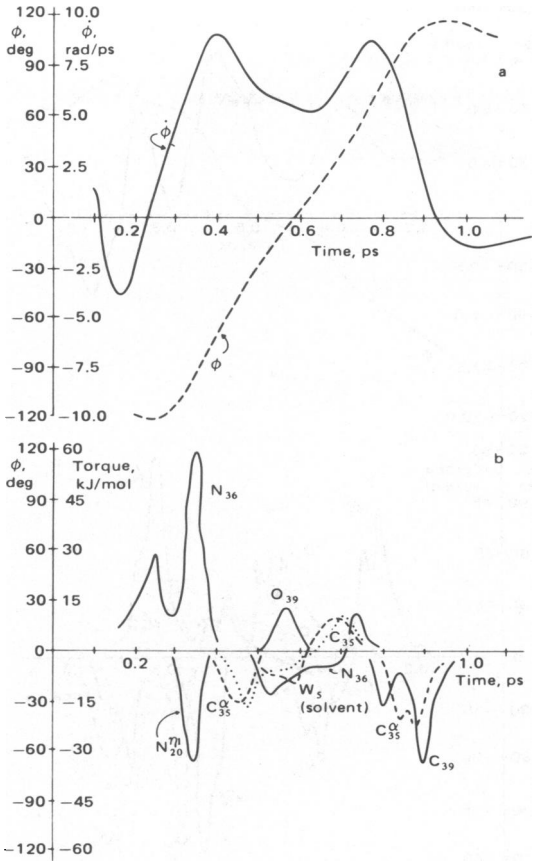

Figure 6 Barrier crossing trajectory of Tyr-35 in a low-density transition region. (*a*) Ring torsion angle (ϕ) and torsional angular velocity ($\dot{\phi}$) as a function of time; (*b*) torques exerted on the ring by particular matrix atoms due to nonbonded interactions (contributions from all atoms for which the repulsion exceeded 0.6 kcal/mol are included).

result is in accord with predictions based on the properties of equilibrium torsional fluctuations of tyrosine rings in PTI, and indicate that transition state theory, with the appropriate choice of reaction coordinate is approximately valid for this rotational isomerization problem. The torsional displacement and angular velocity changes of the ring are well accounted for by the torques acting on the ring due to nonbonded interactions with the surrounding matrix atoms. Many of these torques are sharply peaked functions of time, suggesting that collisional descriptions may be appropriate in first-order analytical models for the barrier-crossing dynamics. The torque impulses are similar to those that occur when the ring oscillates about its equilibrium orientation. The ring is driven over its rotational barrier not as the result of an unusually strong collision, but as the result of a transient decrease in the frequency and intensity of collisions which would tend to drive the ring away from the barrier. This observation suggests that transient packing defects play a role in initiating ring rotation. The local density of the matrix atoms was significantly higher in the first than in the second set of transition states. Correspondingly, frictional effects were somewhat more evident in the first set of trajectories than in the second. This suggests a distinction between "congested"

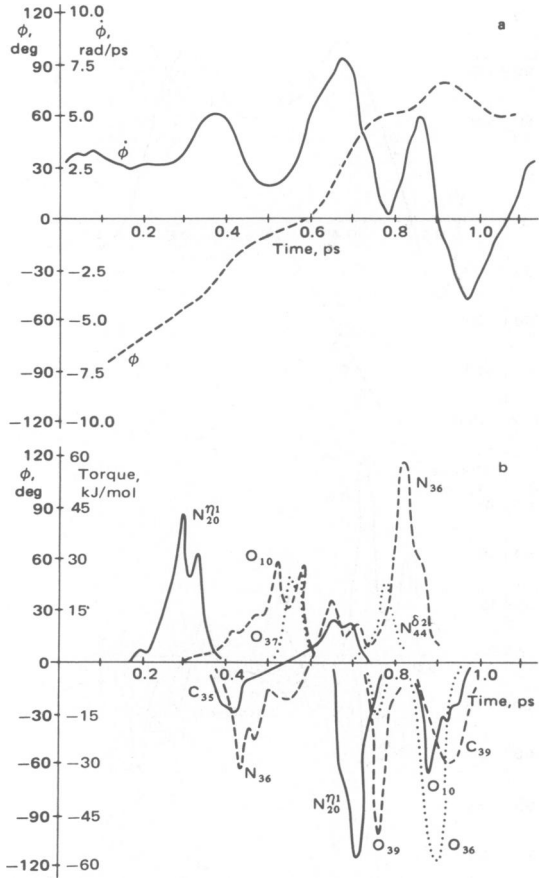

Figure 7 Barrier crossing trajectory of Tyr-35 in a high-density transition region. (*a*) Ring torsion angle (ϕ) and torsional angular velocity ($\dot{\phi}$) as a function of time; (*b*) torques exerted on the ring by particular matrix atoms due to nonbonded interactions (contributions from all atoms for which the repulsion exceeded 0.6 kcal/mol are included).

transition states (in which the local density is high and the ring suffers many collisions as it crosses the barrier) and "uncongested" transition states (in which the opposite is true).

Conclusion

In this paper we have reviewed a number of methods that can be employed to study dynamical processes in proteins. These range from the integration of the equations of motion for an equilibrated protein, an approach best suited for obtaining the short-time fluctuations, to static energy minimizations and phase-space trajectory techniques required for activated processes with significant barriers. Other methods that can be used for appropriate cases include harmonic dynamics, which has recently been applied to the fluctuations of an α-helix (33), and stochastic dynamics, which is being employed in a study of the helix-coil transition (McCammon et al., manuscript submitted for publication) and for relaxation processes in alkanes and amino acid sidechains in solution (34).

Supported in part by grants from the National Science Foundation and the National Institutes of Health and the R. A. Welch Foundation

Received for publication 3 December 1979.

REFERENCES

1. Karplus, M. and J. A. McCammon. 1980. The internal dynamics of globular proteins. *CRC Crit. Rev. Biochem.* In press.
2. Gurd, F. R. N., and T. M. Rothgeb. 1979. Motions in proteins. Adv. in Protein Chem. In press.
3. Case, D. A. and M. Karplus. 1979. Dynamics of ligand binding to heme proteins. *J. Mol. Biol.* **132**:343.
4. Warme, P. K. and H. A. Scheraga. 1974. Refinement of the x-ray structure of lysozyme by complete energy minimization. *Biochemistry.* **13**:757.
5. Levitt, M. 1974. Energy refinement of hen egg-white lysozyme. *J. Mol. Biol.* **82**:393.
6. Gelin, B. R. and M. Karplus. 1975. Sidechains torsional potentials and motion of amino acids in proteins: bovine pancreatic trypsin inhibitor. *Proc. Natl. Acad. Sci. U.S.A.* **72**:2002.
7. Pauling, L., R. B. Corey, and H. R. Branson. 1951. The structure of proteins: two hydrogen-bonded helical configurations of the polypeptide chain. *Proc. Nat. Acad. Sci. U.S.A.* **37**:205.
8. Ramachandran, G. N., C. Ramakrishnan, and V. Sasisekharan. 1963. Stereochemistry of polypeptide chain configurations. *J. Mol. Biol.* **7**:95.
9. Gelin, B. R., and M. Karplus. 1979. Sidechain torsional potentials: effect of dipeptide, protein and solvent environment. *Biochemistry.* **18**:1256.
10. McCammon, J. A., P. G. Wolynes, and M. Karplus. 1979. Picosecond dynamics of tyrosine sidechains in proteins, *Biochemistry.* **18**:927.
11. Schaeffer, H. F., III. 1972. The electronic structure of atoms and molecules. Addison-Wesley, Reading, Mass.
12. Karplus, M., R. N. Porter, and R. D. Sharma. 1965. Exchange reactions with activation energy. I. Simple barrier potential for (H,H_2). *J. Chem. Phys.* **43**:3259.
13. Berne, B. J., Editor. 1977. Modern Theoretical Chemistry, Vol. 6. Plenum Press, New York.
14. McCammon, J. A., B. R. Gelin, and M. Karplus. 1977. Dynamics of folded proteins. *Nature (Lond.).* **267**:585.
15. Gear, C. W. 1971. Numerical initial value problems in ordinary differential equations. Prentice Hall, Englewood, New Jersey.
16. Karplus, M. and J. A. McCammon. 1979. Protein structural fluctuations during a period of 100 ps. *Nature (Lond.).* **277**:578.
17. McQuarrie, D. A. 1976. Statistical mechanics. Harper and Row, New York.
18. Zwanzig, R. 1965. Time-correlation functions and transport coefficients in statistical mechanics. *Ann. Rev. Phys. Chem.*, **16**:67.
19. Chandrasekhar, S. 1943. Stochastic processes in physics and astronomy. *Rev. Mod. Phys.* **15**:1.
20. Synder, G. H., R. Rowan, S. Karplus and B. D. Sykes. 1975. Complete tyrosine assignments in the high field ^1H nuclear magnetic resonance spectrum of the bovine pancreatic trypsin inhibitor. *Biochemistry.* **14**:3765.
21. Wagner, G., A. DeMarco, and K. Wuthrich. 1976. Dynamics of the aromatic amino acid residues in the globular conformation of the basic pancreatic trypsin inhibitor (BPTI). I. ^1H NMR studies. *Biophys. Struct. Mech.* **2**:139.
22. Hetzel, R., K. Wuthrich, J. Deisenhofer and R. Huber. 1976. Dynamics of the aromatic amino acid residues of the globular conformation of the basic pancreatic trypsin inhibitor (BPTI). II. Semi-empirical energy calculations. *Biophys. Struct. Mech.* **2**:159.
23. Austin, R. H., K. W. Beeson, L. Eisenstein, H. Frauenfelder, and I. C. Gunsalus. 1975. Dynamics of ligand binding to myoglobin. *Biochemistry.* **14**:5355.
24. Eisenstein, L. 1977. Dynamics of CO binding to heme proteins. *Int. J. Quant. Chem.: Quant. Biol. Symp.* **4**:363.
25. Knowles, J. R., and W. J. Albery. 1977. Perfection in enzyme catalysis: the energetics of triosephosphate isomerase. *Acc. Chem. Res.* **10**: 105.
26. Warshel, A., and M. Karplus. 1972. Calculation of ground and excited state potential surfaces of conjugated molecules. I. Formulation and parametrization. *J. Am. Chem. Soc.* **94**:5612.
27. Gelin, B. R. and M. Karplus. 1975. Role of structural flexibility in conformational calculations. Application to acetylcholine and β-methyl acetylcholine. *J. Am. Chem. Soc.* **97**:6996.
28. Keck, J. 1962. Statistical investigation of dissociation cross-sections for diatoms. *Discuss. Faraday Soc.* **33**:173.
29. Anderson, J. B. 1973. Statistical theories of chemical reactions. Distribution in the transition region. *J. Chem. Phys.* **58**:4684.
30. Bennett, C. H. 1975. Exact defect calculations in model substances *In* Diffusion in Solids. J.J. Burton and A. S. Nowick, editors. Academic, San Francisco.
31. McCammon, J. A. and M. Karplus. 1979. Dynamics of activated processes in globular proteins. *Proc. Natl. Acad. Sci. U.S.A.* **76**:3585.
32. McCammon, J. A. and M. Karplus. 1980. Dynamics of tyrosine ring rotations in a globular protein. *Biopolymers.* In press.
33. Levy, R. M., and M. Karplus. 1979. Vibrational approach to the dynamics of an α-helix. *Biopolymers* **18**:2465.
34. Levy, R. M., M. Karplus and J. A. McCammon. 1979. Diffusive Langevin dynamics of model alkanes. *Chem. Phys. Letters.* **65**:4.